

MESHFREE NUMERICAL SCHEMES APPLIED TO SEEPAGE PROBLEMS THROUGH EARTH DAMS

Pedro Navas^{1*}, Rena C. Yu², and Susana López-Querol³

¹E.T.S. de Ingenieros de Caminos, Canales y Puertos, UCLM

Avenida Camilo José Cela s/n, 13071 Ciudad Real

E-mail: ¹pedro.navas@uclm.es, ²rena@uclm.es

³School of Computing and Technology, University of West London

St Mary Campus, Ealing, W5 2NU London

E-mail: Susana.Lopez-Querol@uwl.ac.uk

RESUMEN

Modelar la filtración junto con la respuesta mecánica de presas deformables de materiales sueltos sometidas a condiciones transitorias es una tarea compleja, ya que intervienen el acoplamiento entre diferentes fases y el cálculo de variables relacionadas con la superficie libre. En este trabajo se adopta un esquema numérico de métodos sin malla para establecer un marco de resolución del problema acoplado, transitorio, de flujo no confinado en presas de materiales sueltos. Las ecuaciones de Biot son formuladas en desplazamientos (formulación $u - w$), asumiendo medio elástico. Dentro del marco de los métodos sin malla, se han empleado funciones de forma basadas en el principio de Máxima Entropía. La localización de la superficie libre y su evolución en el tiempo se obtienen por interpolación de la presión de poro dentro del dominio. La aplicación a problemas de referencia se ha comparado con resultados disponibles en la literatura

ABSTRACT

Modelling seepage along with the mechanical responses of deformable Earth Dams under transient conditions is a challenging task, since both coupling between different phases, and computation of free-surface variables are involved. In the present work, we take on the meshfree numerical schemes to establish a framework for solving coupled, transient problems for unconfined seepage through Earth Dams. The equations of Biot are formulated in displacement (or $u - w$ formulation) assuming an elastic solid skeleton. Shape functions based on the principle of Maximum Entropy are implemented for the meshfree framework. The free surface location and its evolution in time, is obtained by interpolation of pore water pressures through the domain. Applications to benchmark problems are compared with available results in the literature. The preliminary simulations for steady flow conditions show promising results.

ÁREAS TEMÁTICAS PROPUESTAS: Métodos y Modelos Analíticos y Numéricos

PALABRAS CLAVE: Biot's equations, u-w formulation, Local maximum-entropy

1. INTRODUCTION

The last four decades have seen plenty of numerical development for determining free surface in unconfined seepage problems through porous media. Most of them, however, are formulated in terms of water heads, focusing on the fluid behavior, and tending to neglect the coupling between the fluid phase and the solid skeleton. One exception is the recent u-w formulation by López-Querol *et al.* [1], where a coupling based on displacements of both solid and fluid phases was established. In addition, a procedure to obtain free boundaries through iteratively changing the impermeability boundary conditions was implemented to significantly enhance the calculations.

In this work, we endeavor to apply the meshfree approximation schemes to the seepage problem through earth dams using the u-w formulation. Starting from the development of Arroyo and Ortiz [2], and Sukumar on the principle of maximum entropy [3], as well as the recent thesis of Saucedo [4], we proceed to implement the

equations of Biot [5], and the novel $u - w$ formulation of López-Querol *et al.* [1, 6], instead of the traditional $u - p_w$ formulation to efficiently obtain the free-surface boundaries.

Next we summarize the mathematical framework involved for the $u - w$ displacement formulation, self-adaptive time integration and Max-ent shape functions. The numerical results and comparison with available models are given in Section 3. Finally conclusions and future work are illustrated in Section 4.

2. MATHEMATICAL FRAMEWORK

2.1. Governing equations

The equations of Biot [5] are based on formulating the mechanical behavior of a solid-fluid mixture, the coupling between different phases, and the continuity of flux through a differential domain. For clarity, we use bold symbols for vectors and matrices, normal letters for

scalar variables. Let ρ and ρ_f represent mixture and fluid phase densities; p_w stand for pore water pressure; \mathbf{b} , the external acceleration vector; k , the permeability index (expressed in units $[\text{m}^3][\text{s}]/[\text{kg}]$), the three equations of Biot can be expressed as follows

$$\mathbf{S}^T \mathbf{d}\boldsymbol{\sigma} - \rho \mathbf{d}\ddot{\mathbf{u}} - \rho_f \mathbf{d}\ddot{\mathbf{w}} + \rho \mathbf{d}\mathbf{b} = 0 \quad (1)$$

$$-\nabla dp_w - k^{-1} \mathbf{d}\dot{\mathbf{w}} - \rho_f \mathbf{d}\ddot{\mathbf{u}} - \frac{\rho_f}{n} \mathbf{d}\ddot{\mathbf{w}} + \rho_f \mathbf{d}\mathbf{b} = 0 \quad (2)$$

$$\nabla \cdot \mathbf{d}\dot{\mathbf{w}} + \mathbf{m}^T \mathbf{d}\dot{\boldsymbol{\varepsilon}} + \frac{dp_w}{Q} = 0 \quad (3)$$

where \mathbf{u} is displacement vector of the solid skeleton, and \mathbf{w} the relative displacement of the fluid phase with respect to the solid one. Denoting \mathbf{U} as the absolute displacement of the fluid phase, \mathbf{w} is determined as follows

$$\mathbf{w} = n(\mathbf{U} - \mathbf{u}) \quad (4)$$

where n is the porosity of the soil. In addition, Q in Eqs. (1-3) is the volumetric compressibility of the mixture, and \mathbf{S} represents a matrix operator, which, in 2D problems, is defined as:

$$\mathbf{S} = \begin{pmatrix} \frac{\partial}{\partial x} & 0 \\ 0 & \frac{\partial}{\partial y} \\ \frac{\partial}{\partial y} & \frac{\partial}{\partial x} \end{pmatrix} \quad (5)$$

In Eq. (3), \mathbf{m} is the unit matrix expressed in Voigt form, which in 2D reads

$$\mathbf{m} = \begin{pmatrix} 1 \\ 1 \\ 0 \end{pmatrix} \quad (6)$$

Assuming tensile stresses and strains as positive, whereas compression for pore water pressure p_w , the Terzaghi's effective stress [7] is defined as follows

$$\boldsymbol{\sigma}' = \boldsymbol{\sigma} - p_w \mathbf{m} \quad (7)$$

where $\boldsymbol{\sigma}'$ and $\boldsymbol{\sigma}$ are the respective vectorial form in Voigt notation for the effective and total stress tensor.

If linear elasticity is assumed, the relationship between stresses and strains, expressed in its incremental form, is governed by:

$$\mathbf{d}\boldsymbol{\sigma}' = \mathbf{D}^e \mathbf{d}\boldsymbol{\varepsilon} \quad (8)$$

where \mathbf{D}^e denotes the elastic tensor. Under plane strain conditions, it is given by:

$$\mathbf{D}^e = \frac{\lambda}{\nu} \begin{pmatrix} 1 - \nu & \nu & 0 \\ \nu & 1 - \nu & 0 \\ 0 & 0 & \frac{1 - 2\nu}{2} \end{pmatrix} \quad (9)$$

where ν is the Poisson's ratio, λ the first constant of Lamé.

Rearranging the above equations, Eq. (1) can be rewritten as

$$\mathbf{S}^T \mathbf{D}^e \mathbf{S} \mathbf{d}\mathbf{u} - \nabla dp_w - \rho \mathbf{d}\ddot{\mathbf{u}} - \rho_f \mathbf{d}\ddot{\mathbf{w}} + \rho \mathbf{d}\mathbf{b} = 0 \quad (10)$$

Next we explain in detail the $u - w$ formulation in order to solve the governing equations Eq. (10) and Eqs.(2-3).

2.2. $u-w$ formulation

The $u - w$ approach, also known as the *complete* formulation, since no additional assumption is required under plain strain conditions, each node has five degrees of freedom, u and w (two components each in 2D) and the scalar p_w , see [1] for details. By comparison, the traditional $u - p_w$ formulation, each node has only three degrees of freedom in 2D, but results the disadvantage of neglecting the term $d\ddot{w}$.

Integrating Eq. (3) in time, and substituting dp_w in Eqs. (10) and (2), we have

$$\begin{aligned} \mathbf{S}^T \mathbf{D}^e \mathbf{S} \mathbf{d}\mathbf{u} + Q \nabla (\nabla^T \mathbf{d}\mathbf{u}) + Q \nabla (\nabla^T \mathbf{d}\mathbf{w}) \\ - \rho \mathbf{d}\ddot{\mathbf{u}} - \rho_f \mathbf{d}\ddot{\mathbf{w}} + \rho \mathbf{d}\mathbf{b} = 0 \end{aligned} \quad (11)$$

$$\begin{aligned} Q \nabla (\nabla^T \mathbf{d}\mathbf{u}) + Q \nabla (\nabla^T \mathbf{d}\mathbf{w}) - k^{-1} \mathbf{d}\dot{\mathbf{w}} \\ - \rho_f \mathbf{d}\ddot{\mathbf{u}} - \frac{\rho_f}{n} \mathbf{d}\ddot{\mathbf{w}} + \rho_f \mathbf{d}\mathbf{b} = 0 \end{aligned} \quad (12)$$

The final system of equations, once the element matrices have been assembled, can be expressed as:

$$\mathbf{K} \mathbf{d}\mathbf{u} + \mathbf{C} \mathbf{d}\dot{\mathbf{u}} + \mathbf{M} \mathbf{d}\ddot{\mathbf{u}} = \mathbf{d}\mathbf{f} \quad (13)$$

where \mathbf{K} , \mathbf{C} and \mathbf{M} respectively denote stiffness, damping and mass matrices, $\mathbf{d}\mathbf{u}$ represents the vector of unknowns, expressed incrementally, and $\mathbf{d}\mathbf{f}$ is the increment of the external forces vector, containing gravity acceleration, as well as boundary conditions for nodal forces.

2.3. Time integration scheme

To solve the system of equations shown in (13) in the time domain, the step-by-step Newmark's time integration scheme has been adopted [8]. The method consists of dividing the time domain into steps, with time interval Δt , small enough to warrant both convergence and accuracy of the solution. If the current time step is numbered as $n + 1$, and assuming the solution in the previous step n

has been already obtained (and hence it is known), a relationship between \mathbf{u}_{n+1} , $\dot{\mathbf{u}}_{n+1}$ and $\ddot{\mathbf{u}}_{n+1}$ is established according to a finite different scheme, as follows:

$$\ddot{\mathbf{u}}_{n+1} = \ddot{\mathbf{u}}_n + \Delta\ddot{\mathbf{u}}_{n+1} \quad (14)$$

$$\dot{\mathbf{u}}_{n+1} = \dot{\mathbf{u}}_n + \ddot{\mathbf{u}}_n\Delta t + \beta_1\Delta t\Delta\ddot{\mathbf{u}}_{n+1} \quad (15)$$

$$\begin{aligned} \mathbf{u}_{n+1} = & \mathbf{u}_n + \dot{\mathbf{u}}_n\Delta t + \frac{1}{2}\Delta t^2\ddot{\mathbf{u}}_n \\ & + \frac{1}{2}\beta_2\Delta t^2\Delta\ddot{\mathbf{u}}_{n+1} \end{aligned} \quad (16)$$

where β_1 and β_2 are coefficients. To ensure stability, the following condition needs to be enforced

$$\beta_2 \geq \beta_1 \geq 0.5$$

We choose β_1 and β_2 to be 0.6 and 0.605 respectively to improve the stability and convergence by allowing a small numerical damping.

Rearranging the above expressions, Eq. (13) finally yields

$$\begin{aligned} & \left[\frac{2}{\beta_2\Delta t^2}\mathbf{M} + \frac{2\beta_1}{\beta_2\Delta t}\mathbf{C} + \mathbf{K} \right] \Delta\mathbf{u}_{n+1} = \\ & d\mathbf{f}_{n+1} + \left[\frac{2}{\beta_2\Delta t}\mathbf{M} + \frac{2\beta_1}{\beta_2}\mathbf{C} \right] \dot{\mathbf{u}}_n \\ & + \left[\frac{1}{\beta_2}\mathbf{M} - \Delta t \left(1 - \frac{\beta_1}{\beta_2} \right) \mathbf{C} \right] \ddot{\mathbf{u}}_n \end{aligned} \quad (17)$$

A self-adaptive procedure, proposed in [9] is implemented to select the correct time step, keeping the total numerical error under a given limit. Using a given time interval Δt , the numerical error e_u is defined as:

$$e_u = \left\| \frac{1}{2}\Delta t^2 \left(\beta_2 - \frac{1}{3} \right) \Delta\mathbf{u}_{n+1} \right\| \quad (18)$$

where $\|\cdot\|$ represents the norm of the vector inside. Once this error has been obtained, the new time step adapts according to the following condition

$$\frac{\Delta t_{new}}{\Delta t_{old}} = \begin{cases} 1 & \text{if } \frac{e_u}{e^*} \in [0.2, 2] \\ \left[\frac{e^*}{e_u} \right]^{1/3} & \text{otherwise} \end{cases} \quad (19)$$

where e^* is the error tolerance set as 5×10^{-6} .

2.4. Spatial discretization: Max-ent shape functions

The basic idea of the shape functions based on the principle of maximum entropy is to interpret the shape function $N^a(\mathbf{x})$ as the probability of \mathbf{x} to obtain the value \mathbf{x}^a . Taking Shannon's entropy as a starting point:

$$H(p_1(\mathbf{x}), \dots, p_n(\mathbf{x})) = - \sum_{a=1}^N p_a(\mathbf{x}) \log p_a \quad (20)$$

where $p_a(\mathbf{x})$ is the probability and is equivalent to the mentioned shape function $N_a(\mathbf{x})$, satisfying the zeroth and first-order consistency.

The least-biased approximation scheme is given by

$$\begin{aligned} \text{(ME) Maximize } H(\mathbf{p}) &= - \sum_{a=1}^N p_a(\mathbf{x}) \log p_a \\ \text{subject to } p_a &\geq 0, \quad a=1, \dots, n \\ \sum_{a=1}^N p_a &= 1 \\ \sum_{a=1}^N p_a \mathbf{x}_a &= \mathbf{x} \end{aligned}$$

The local max-ent approximation schemes as a Pareto set defined by Arroyo and Ortiz [2] is as follows

(LME) $_{\beta}$ For fixed \mathbf{x} minimize

$$\begin{aligned} f_{\beta}(\mathbf{x}, \mathbf{p}) &= \beta H(\mathbf{x}, \mathbf{p}) - H(\mathbf{p}) \\ \text{subject to } p_a &\geq 0, \quad a=1, \dots, n \\ \sum_{a=1}^N p_a &= 1 \\ \sum_{a=1}^N p_a \mathbf{x}_a &= \mathbf{x} \end{aligned}$$

where $\beta \in (0, \infty)$ is Pareto optimal.

The unique solution of the local max-ent problem (LME) $_{\beta}$ is:

$$p(\mathbf{x}) = \frac{\exp[-\beta|\mathbf{x} - \mathbf{x}_a|^2 + \lambda(\mathbf{x} - \mathbf{x}_a)]}{Z(\mathbf{x}, \lambda^*(\mathbf{x}))} \quad (21)$$

where

$$Z(\mathbf{x}, \lambda) = \sum_{a=1}^N \exp[-\beta|\mathbf{x} - \mathbf{x}_a|^2 + \lambda(\mathbf{x} - \mathbf{x}_a)] \quad (22)$$

and $\lambda^*(x)$ is the unique maximizer of

$$g(\lambda) = -\log\{Z(\mathbf{x}, \lambda)\} \quad (23)$$

The geometric interpretation given in [4] allows us to solve the problem without the logarithm function, since Z and $\log[Z]$ obtain their minimums at the same location, see Fig. 1

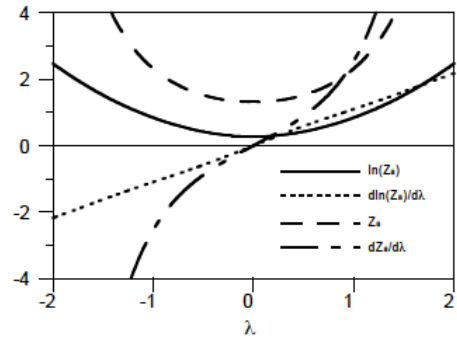


Figure 1: Comparison of the location of the minimum with and without logarithm in 1D.

In order to obtain the first derivatives of the shape function, it is also necessary to compute ∇p_a^*

$$\nabla p_a^* = p_a^* \left(\nabla f_a^* - \sum_b p_a^* \nabla f_a^* \right) \quad (24)$$

where

$$f_a^*(\mathbf{x}, \lambda, \beta) = -\beta |\mathbf{x} - \mathbf{x}_a|^2 + \lambda(\mathbf{x} - \mathbf{x}_a) \quad (25)$$

Deriving by the chain rule, rearranging and considering β as constant, Arroyo and Ortiz [2] obtained the following expression:

$$\nabla p_a^* = -p_a^*(\mathbf{J}^*)^{-1}(\mathbf{x} - \mathbf{x}_a) \quad (26)$$

where

$$\mathbf{J}(\mathbf{x}, \lambda, \beta) = \frac{\partial \mathbf{r}}{\partial \lambda} \quad (27)$$

$$\mathbf{r}(\mathbf{x}, \lambda, \beta) = \sum_a p_a(\mathbf{x}, \lambda, \beta)(\mathbf{x} - \mathbf{x}_a) \quad (28)$$

where p_a is ranged between $-\infty$ and ∞ . In practice, it is calculated between two limit values r_1 and r_2 , when f_a reaches a given tolerance, as shown in Fig. 2.

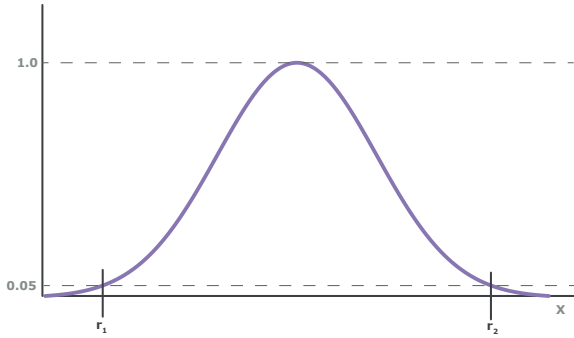


Figure 2: Limit values r_1 and r_2 which give an f_a value of 0.05.

The limit values for r_1 and r_2 are calculated as follows:

$$\exp[f_a(\mathbf{r}, \beta)] = \exp[-\beta r_i^2] = \text{tol} \Rightarrow$$

$$r_i = \sqrt{-\frac{\ln(\text{tol})}{\beta}}, \quad i = 1 \text{ or } 2 \quad (29)$$

This limit value is used thereafter to find the neighbor nodes of a given integration point.

2.5. Determination of the free boundary (or phreatic surface)

There are two basic methods to determine the free boundary in an unconfined flow system. One is through dra-

wing trial flow net, the other is employing numerical solutions based on parabola. For example, the Dupuit solution [10] assumes that flow lines are nearly horizontal and the hydraulic gradient of the flow is equal to the slope of the phreatic surface, but it does not take into account neither the slope geometry nor the entrance and exit conditions.

Here we choose the procedure developed by López-Querol *et al.* [1], which obtains the sought phreatic surface by imposing Dirichlet boundary conditions for the fluid phase. This is possible thanks to the employed displacement formulation, since there is no water displacement at those boundaries. As such surface is unknown at the beginning of the calculation, the impermeability condition at downstream is necessarily changed by allowing water displacement below the free surface. The iterative procedure finishes when there is no need to change the impermeability boundary conditions, which typically occurs after 4 or 5 iterations.

3. NUMERICAL RESULTS

In this Section, we apply the aforementioned methodology to two benchmark problems in Soil Mechanics, the Muskat problem and the Drain toe rectangular dam. Then we compare the obtained results with available ones in the literature.

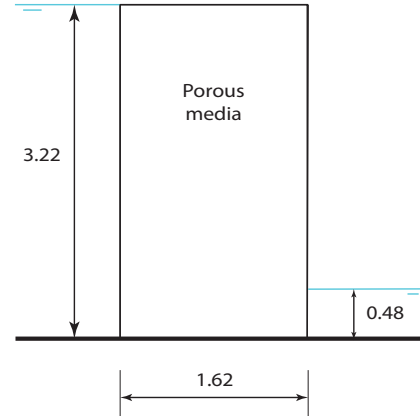


Figure 3: Geometry of the Muskat problem (units in m).

3.1. Muskat problem

The Muskat problem is originally defined as the dynamics of the interface between two incompressible immiscible fluids with different constant densities. Within the framework of soil mechanics, it is the evolution of the phreatic surface in a homogeneous rectangular earth

dam. The porous rectangular dam is above a horizontal impermeable base. There is a steady flow in which water seeps through the dam from one reservoir (one the left, 3.22 m) to a lower one (on the right, 0.48 m). Because of gravity, the water does not flow through the entire dam, thus it is dry near its upper-right corner. The interface separating the dry and wet regions of the dam is a free boundary.

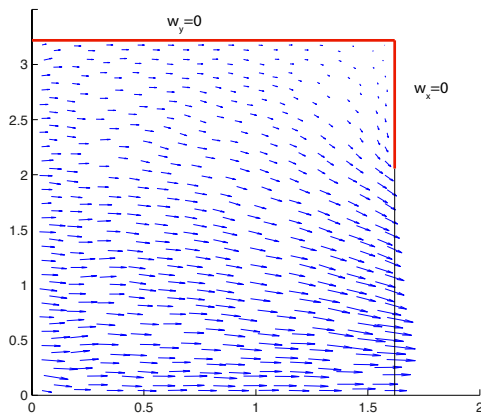


Figura 4: Final iteration of Muskat problem and boundary conditions on upper-right corner.

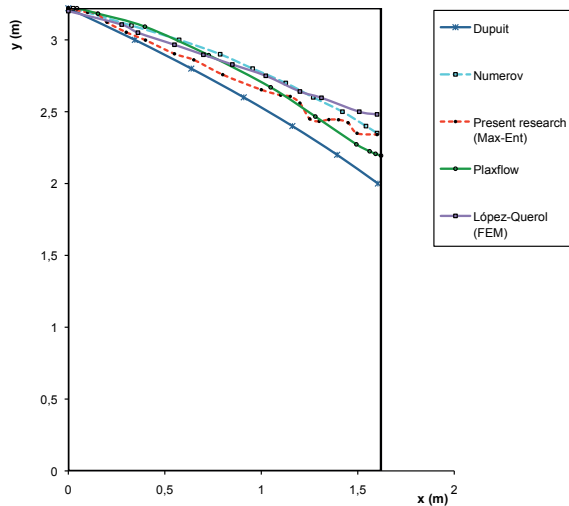


Figura 5: Comparison of the obtained phreatic surface with that from Dupuit, Numerov, Plaxiflow and López-Querol.

The resulted boundary conditions and water flux (or velocity field) are shown in Fig. 4. In Fig. 5, we compare the obtained phreatic surface profile with that of Dupuit, Numerov [11], the commercial software Plaxiflow [12], as well as the finite element solution of López-Querol *et al.* [1]. Note that the proposed meshfree methodology captures the main trend of the free boundary, but there

exists certain instability at the downstream side. We attribute it to the directional feature of the employed shape function, which improvement is under way.

3.2. Drain toe in a rectangular Earth dam

The problem of drain toe in a theoretical, rectangular, homogeneous Earth dam was first presented by Borja and Kishnani [13]. They applied hydrostatic forces caused by the water level to the dam at its up and downstream boundaries. Navas and López-Querol [6] recently carried out a study on the same problem through the iterative procedure described in Section 2.5. We compare the obtained free boundary with that of [13, 6] in Fig. 6. Note that the accuracy of the proposed mesh-free methodology is similar to that of the Muskat problem. Despite the instability near the toe drain, the solution is close to the one obtained in [6] through finite element calculations.

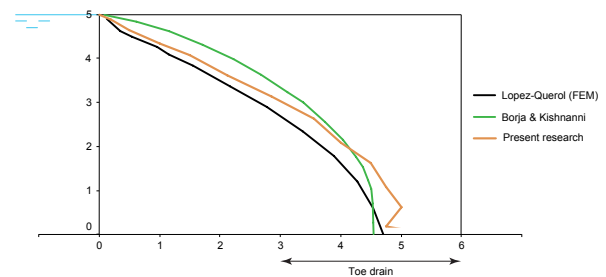


Figura 6: Comparison of the obtained free boundary for the Drain toe in a rectangular Earth dam

4. CONCLUSIONS

We have implemented the $u - w$ formulation for Biot's equation under the meshfree framework. The shape functions are based on the principle of Maximum Entropy. Self-adaptive integration schemes are chosen to balance both accuracy and efficiency. The proposed procedure are applied to study the Muskat problem and the drain toe in a rectangular Earth dam. The preliminary result seems promising even though improvements should be carried out in resolving observed instabilities.

ACKNOWLEDGEMENTS

We acknowledge the financial support from the *Ministerio de Ciencia e Innovación*, BIA2012-31678 and MAT2012-35426, Spain.

REFERENCIAS

- [1] S. López-Querol, P. Navas, J. Peco, and J. Arias-Trujillo. Changing impermeability boundary conditions to obtain free surfaces in unconfined seepage problems. *Canadian Geotechnical Journal*, 48:841–845, 2011.

- [2] M. Arroyo and M. Ortiz. Local maximum-entropy approximation schemes: a seamless bridge between finite elements and meshfree methods. *International Journal for Numerical Methods in Engineering*, 65(13):2167–2202, 2006.
- [3] A. Ortiz, M.A. Puso, and N. Sukumar. Maximum-entropy meshfree method for compressible and near-incompressible elasticity. *Computer Methods in Applied Mechanics and Engineering*, 199:1859–1871, 2010.
- [4] L. Saucedo. *Meshfree methods applied to tensile fracture and compressive damage in quasi-brittle materials*. PhD thesis, Universidad de Castilla-La Mancha, 2012.
- [5] M. A. Biot. Theory of propagation of elastic waves in a fluid-saturated porous solid. I. Low-Frequency range. *Journal of the Acoustical Society of America*, 28(2):168–178, 1956.
- [6] P. Navas and S. López-Querol. Generalized unconfined seepage flow model using displacement based formulation. *Engineering Geology*, 166:140–141, 2013.
- [7] K. V. Terzaghi. Principles of Soil Mechanics. *Engineering News-Record*, 95:19–27, 1925.
- [8] N.M. Newmark. A method of computation for structural dynamic. *Journal of the Engineering Mechanics Division - ASCE*, 85:67–94, 1959.
- [9] J.A. Fernández-Merodo. *Une approche a la modelization des glissements et des effondrements de terrains: initiation et propagation (in French)*. PhD thesis, Ecole Centrale des Arts et Manufactures“Ecole Centrale Paris”, 2001.
- [10] G. Keady. The Dupuit approximation for the rectangular dam problem. *IMA Journal of Applied Mathematics*, 44:243–260, 1990.
- [11] M.E. Harr. *Groundwater and seepage*. McGraw-Hill, Inc., New York, 1962.
- [12] Plaxis. *PLAXFLOW validation manual*. Delft, the Netherlands, version 1.4 edition, 2010. Available from www.plaxis.nl.
- [13] R.I. Borja and S.S. Kishnani. On the solution of elliptic free-boundary problems via Newton’s method. *Computer Methods in Applied Mechanics and Engineering*, 88:341–361, 1991.